Earth and Planetary Science Letters 447 (2016) 103–111

Contents lists available at ScienceDirect

Earth and Planetary Science Letters

www.elsevier.com/locate/epsl

Atmospheric nitrogen evolution on Earth and Venus

R.D. Wordsworth [a,b,*]

[a] Harvard Paulson School of Engineering and Applied Sciences, Harvard University, Cambridge, MA 02138, United States
[b] Department of Earth and Planetary Sciences, Harvard University, Cambridge, MA 02138, United States

ARTICLE INFO

Article history:
Received 8 September 2015
Received in revised form 25 March 2016
Accepted 3 April 2016
Available online 13 May 2016
Editor: C. Sotin

Keywords:
nitrogen
atmosphere
mantle
photochemistry
redox
Venus

ABSTRACT

Nitrogen is the most common element in Earth's atmosphere and also appears to be present in significant amounts in the mantle. However, its long-term cycling between these two reservoirs remains poorly understood. Here a range of biotic and abiotic mechanisms are evaluated that could have caused nitrogen exchange between Earth's surface and interior over time. In the Archean, biological nitrogen fixation was likely strongly limited by nutrient and/or electron acceptor constraints. Abiotic fixation of dinitrogen becomes efficient in strongly reducing atmospheres, but only once temperatures exceed around 1000 K. Hence if atmospheric N_2 levels really were as low as they are today 3.0–3.5 Ga, the bulk of Earth's mantle nitrogen must have been emplaced in the Hadean, most likely at a time when the surface was molten. The elevated atmospheric N content on Venus compared to Earth can be explained abiotically by a water loss redox pump mechanism, where oxygen liberated from H_2O photolysis and subsequent H loss to space oxidises the mantle, causing enhanced outgassing of nitrogen. This mechanism has implications for understanding the partitioning of other Venusian volatiles and atmospheric evolution on exoplanets.

Despite the fact that it makes up over 78% of our atmosphere and is essential to all known life, nitrogen remains a poorly understood element on Earth. In comparison to other major non-metal elements such as oxygen and carbon, the mechanisms responsible for its initial delivery, isotopic evolution and partitioning between the surface and mantle are all still subject to great uncertainty. As a result, one of the most basic features of our planet's climate – the atmospheric pressure – remains unexplained by Earth science.

Nitrogen is an important player in climate because it causes pressure broadening of the absorption lines of greenhouse gases like CO_2 and H_2O (Goldblatt et al., 2009), and can also cause intense warming in combination with H_2 in reducing atmospheres via collision-induced absorption in the 800–1200 cm^{-1} H_2O 'window' region of the infrared spectrum (Wordsworth and Pierrehumbert, 2013). The atmospheric nitrogen inventory also affects the latitudinal temperature gradient (in general denser atmospheres transport heat from equator to poles more effectively). All these effects are particularly relevant in the context of the faint young Sun problem, which arises because solar luminosity was 20–25% lower 3–4 Ga, but Earth was not permanently glaciated in the Archean (Sagan and Mullen, 1972). Furthermore, planets with very low atmospheric N_2 will no longer cold trap H_2O and hence will irreversibly oxidise via hydrogen loss, which can lead to the buildup of abiotic O_2-dominated atmospheres in extreme cases (Wordsworth and Pierrehumbert, 2014). Understanding Earth's nitrogen is hence important both as a fundamental problem, and for addressing wider questions of planetary climate evolution.

Thanks to its strong triple bond and lack of a permanent dipole moment, molecular nitrogen (N_2) is both chemically unreactive and highly volatile, and hence was once thought of as similar to the noble gases in terms of its incompatibility in the solid Earth. However, this simple view of N_2 has been eroded over the last few decades by a number of studies suggesting that a significant fraction of the present-day atmospheric inventory (between around 0.4 and 7 times) is currently stored in the crust and mantle (Marty, 1995; Marty and Dauphas, 2003; Halliday, 2013; Johnson and Goldblatt, 2015). The main evidence for this comes from the $N_2/^{40}Ar$ ratios measured in mid-ocean ridge basalts (MORBs) and rocks of mantle plume origin, which allow the mantle N inventory to be estimated when combined with bulk silicate Earth (BSE) estimates of radiogenic K abundance. Earth's atmosphere is also depleted in ^{14}N relative to chondritic C and noble gas abundance ratios (Marty, 2012) (the 'missing N' problem), which can be explained by the presence of a substantial mantle N component (Johnson and Goldblatt, 2015). The correlation of N with ^{40}Ar in MORBs and the large-ion lithophile elements

* Correspondence to: Harvard Paulson School of Engineering and Applied Sciences, Harvard University, Cambridge, MA 02138, United States.
E-mail address: rwordsworth@seas.harvard.edu.

http://dx.doi.org/10.1016/j.epsl.2016.04.002
0012-821X/

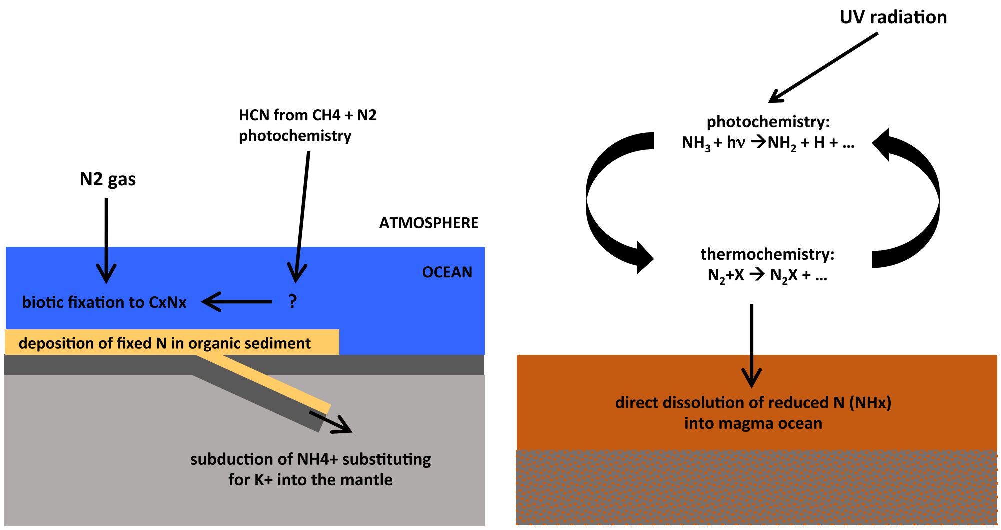

Fig. 1. (left) Biological and (right) abiotic mechanisms capable of transferring atmospheric nitrogen to early Earth's mantle. Biological mechanisms are possible from the origin of nitrogen fixation and methanogenesis metabolisms onwards, while the abiotic mechanism shown would have operated in the early Hadean, during and just after accretion.

in metamorphic rocks also suggests that its primary form in the crust and upper mantle is NH_4^+, where it generally substitutes for K^+ (Busigny and Bebout, 2013). Finally, measurements of the content of nitrogen and other volatiles in Alpine metasediments suggest that today, there is a net flux of N to the mantle of order 1×10^{12} g/yr (Busigny and Bebout, 2013).

Based on these observations, it has been proposed that biological N fixation has caused atmospheric nitrogen levels to decrease over geological time, and hence that surface pressure on the early Earth was two times or more the present-day value (Goldblatt et al., 2009). However, this apparently logical conclusion has not been supported by recent observational constraints on the ancient atmospheric pressure. First, measurements of the radii of putative fossil raindrops have been argued to constrain the atmospheric density 2.7 Ga to no more than double the present-day value (Som et al., 2012). Independently, recent measurements of N_2 to ^{36}Ar ratios in the fluid inclusions in Archean hydrothermal quartz have suggested that as long ago as 3.0–3.5 Ga, the partial pressure of N_2 in the atmosphere was 0.5–1.1 bar (Marty et al., 2013). Hence Earth's mantle N inventory was apparently in place by the mid-Archean or earlier. If these measurements are correct, nitrogen exchange between the mantle and interior must have been very effective at some earlier point in Earth's early history.

Further clues to terrestrial nitrogen's origins and evolution come from isotopic measurements. Of nitrogen's two stable isotopes, the rarer ^{15}N is enhanced in the atmosphere and in crustal rocks relative to the mantle [δ^{15}N of approx. -5‰ vs. the atmosphere in the upper mantle and perhaps as low as -40‰ in the lower mantle; Cartigny and Marty, 2013].[1] This has been interpreted previously as an indication of biological processes. Earth's atmospheric $^{15}N/^{14}N$ ratio ($\sim 3.7 \times 10^{-3}$) is close to the values found in ordinary and carbonaceous chondrites (Marty, 2012), but the solar and gas giant N reservoirs are lighter ($\sim 2.3 \times 10^{-3}$; Owen et al., 2001). This has led to the prevailing view that most of Earth's N was delivered by bodies with composition close to that of the carbonaceous chondrites. At which stage of accretion, and in what form this nitrogen was delivered is still uncertain, but a reasonable interpretation is of volatile-rich bodies of chondritic composition impacting the Earth during the later stages of accretion, with much of the nitrogen in the form of ammonia ices or simple organic compounds such as HCN.

Clearly, our current understanding of the long-term atmosphere-interior exchange of nitrogen on Earth is lacking in many respects. Most previous research has focused on improving the (vital) geochemical constraints on the deep-time N cycle. To date, however, far less attention has been paid to the theoretical aspects of the problem. Here the importance of several key processes to Earth's earliest nitrogen cycle are analysed (see Fig. 1). First, it is noted that nitrogen delivered to Earth in fixed form would have initially degassed into the atmosphere and that it therefore must have entered the mantle at some point after this. Based on primary productivity constraints and other arguments, it is then argued that drawdown of bars of nitrogen before 3.0–3.5 Ga via biological fixation is highly unlikely. An atmospheric chemistry model is used to show that abiotic reduction of atmospheric nitrogen can be effective, but only under conditions where the atmosphere is strongly reducing and the surface temperature is extremely hot. Based on this, a new explanation involving a magma ocean redox pump driven by water loss is proposed for the differing atmospheric N inventories of Earth and Venus.

1. Nitrogen delivery by impacts

The first stage of Earth's nitrogen cycle is delivery of the element during accretion. As discussed in the introduction, most of this incoming nitrogen was likely fixed in the form of ammonia ices or organics. However, the temperatures and peak shock pressures on impact for the majority of accreting bodies mean that it would have initially thermalised and degassed into the atmosphere. Impact shock experiments on carbonaceous chondrites (Tyburczy et al., 1986) indicate that for accretion occurring after Earth has reached around 30% of its final radius, mineral devolatilisation is effective. As the majority of Earth's nitrogen was probably delivered late, this implies the immediate post-impact location of delivered nitrogen would have been the atmosphere. Note that as well as depositing their own nitrogen to the atmosphere, impactors would also devolatilise any crustal and sedimentary nitrogen that was already present in the region of impact. We do not attempt to model this process here, but it would act to reduce the efficiency of the slow drawdown mechanisms discussed in the next two sections.

[1] Here for a given sample i, $\delta^{15}N = 1000[(^{15}N/^{14}N)_i/(^{15}N/^{14}N)_{atm} - 1]$ and $(^{15}N/^{14}N)_{atm} = 3.7 \times 10^{-3}$ is the Earth atmospheric value.

2. Direct biological nitrogen fixation

If most or all of the N currently in the bulk silicate Earth started in the atmosphere, some mechanism must be responsible for depositing it in the mantle over time. The simplest explanation for the origin of Earth's mantle N is the same process that is apparently producing a net subduction flux of nitrogen today: biological N fixation. Is this likely to have been important throughout geologic time? If the present-day flux were constant throughout Earth's history, 22–35% of the present-day atmospheric inventory would have been drawn down between the cooling of Earth's surface after the Moon-forming impact 4.4 Ga (the earliest possible date for the origin of life) and 3.0–3.5 Ga, when recent studies (Marty et al., 2013) argue for close to present-day atmospheric levels of N_2. Clearly, higher subduction fluxes in the past are required to explain the current mantle N inventory.

Several effects could have altered the biogenic flux of fixed N to subduction zones with time. In the oceans today, the molar ratio of N to C in organic matter is approximately 1:6.6 (the Redfield ratio). In the past, this ratio might have been slightly different due to e.g. variations in the contribution of protein to the total biomass (Geider and La Roche, 2002). However, it is highly unlikely to have decreased below around 1:4, due to fundamental amino acid stoichiometry.

Changes in the rates of sediment nitrogen loss prior to subduction are harder to constrain. Under anoxic conditions, conversion of fixed N to nitrate and hence denitrification rates would clearly have been less efficient than today. However, ammonification of organic nitrogen would still have provided the biosphere with an efficient mechanism to return reduced N to the ocean and atmosphere. Furthermore, fixed N is energetically costly, so an early biosphere with a much greater organic N:C loss ratio than today would contain strong incentives for the development of efficient sediment N removal pathways if they did not exist initially.

If the N:C ratio in sediment did not change significantly in the past, what about the total rate of subduction of organics? Simple interpretations of the isotopic record of sedimentary carbon imply that organic carbon burial rates were around 10% of the total in the Archean, compared to around 20% today (Des Marais et al., 1992). Seafloor carbonisation and authigenic carbonate formation (Bjerrum and Canfield, 2004; Schrag et al., 2013), which are both poorly constrained, would decrease this percentage further if they were significant in Earth's early history.

Lower Archean organic carbon burial rates make sense even if oxygenic photosynthesis emerged early, because nutrient supply to the biosphere in the Archean was probably lower than today. The present-day net primary productivity (NPP) of the marine biosphere is limited on long timescales by the supply of phosphorous (Filippelli, 2008). The dependence of phosphorous supply on land weathering means that the area of exposed land is a key factor controlling primary productivity. In the Archean the continents were still forming, with estimates of the amount of emergent land 3.5 Ga ranging between 3 and 30% (Flament et al., 2008; Dhuime et al., 2012). This implies decreased P supply to the oceans (Wordsworth and Pierrehumbert, 2013). In addition, abiotic sinks for P are probably higher in anoxic environments (Bjerrum and Canfield, 2002).

Perhaps the most important point regarding biological N fixation in the Archean, however, is that today's biosphere is powered by oxygenic photosynthesis. The date when this key metabolism emerged is not known, but there is no strong evidence that it existed 3.0 Ga or earlier. This is crucial, because before the advent of oxygenic photosynthesis primary productivity must have been drastically lower. Ecological models (Kharecha et al., 2005) predict that in an ecosystem dominated by methanogenesis, NPP was lower than today by a factor of 500–3000. Under these circumstances, burial rates of biologically fixed N would have to be significantly lower as well. Substantial nitrogen subduction due to direct biological fixation in the early Archean and Hadean therefore appears unlikely.

3. Photochemical nitrogen fixation

If methanogens emerged prior to oxygenic photosynthesis, there was probably a period when atmospheric methane levels were high (Pavlov et al., 2003). Then, HCN formation via reactions of the type

$$^{3}CH_2 + N(^{4}S) \rightarrow HCN + H \tag{1}$$

in the upper atmosphere could potentially have led to rapid N fixation. Reaction (1), which was first studied in a planetary atmospheric context by Yung et al. (1984), has been proposed as an important source of HCN for prebiotic chemistry in Earth's early atmosphere (Zahnle, 1986). Given sufficient quantities of atmospheric methane, it could have led to N fixation rates of up to 1×10^{10} molecules/cm^2/s (Tian et al., 2011). In the absence of any recycling, this would be sufficient to remove Earth's entire present-day nitrogen inventory in around 100 Myr (Tian et al., 2011; Wordsworth and Pierrehumbert, 2013).

In the context of bulk N drawdown, the advantage of atmospheric HCN formation over surface biological fixation of N is that the rate of methane production in a biosphere dominated by methanogens and/or anoxygenic photosynthesis is many times greater than the NPP (Kharecha et al., 2005). Could this provide an alternative route to drawdown of the nitrogen in the early atmosphere?

To work before 3.0–3.5 Ga, this mechanism clearly requires either methanogens or anoxygenic phototrophs (or both) to have created a globally significant biosphere very early on. This is possible, as methanogenesis is believed to be an ancient metabolism, although phyllogenetic molecular clock estimates of the date of mesophilic methanogen emergence range from 3.8 to 1.3 Ga (Battistuzzi et al., 2004; Blank, 2009). The high HCN production rates needed to achieve rapid N drawdown also require extremely high atmospheric methane levels (~1000 ppmv). Besides a thriving methanogen ecosystem, this requires a combination of high hydrogen outgassing and seafloor serpentinization rates and/or low hydrogen escape rates.

Finally, once it reaches the surface, the photochemically produced HCN must still be incorporated into sediment. The most logical way for this to occur is by biological conversion to ammonia (e.g., as occurs via certain fungi and bacteria today; Knowles, 1988), followed by incorporation into organic matter. However, the biosphere would be unlikely to incorporate nitrogen into organic material at a rate greater than that required by the NPP, which in a fixed-N-rich environment would probably be P-limited. Then, the restrictions on N burial based on availability of nutrients and/or electron donors discussed in the last section would again apply. Even if the biosphere were able to incorporate all the available nitrogen from HCN, the conversion efficiency from HCN to NH_3 to organic matter would need to be high, because gaseous ammonia is highly unstable to dissociation by photolysis in the atmosphere next section. Hence rapid drawdown of N before 3.0–3.5 Ga by this mechanism also appears challenging to achieve. For this reason, we now turn to abiotic processes that could have been important in the Hadean.

4. N_2 thermolysis in a highly reducing atmosphere

In the Hadean, atmospheric and crustal conditions would have been far more reducing than later on, due to processes such as nebular capture (Genda and Ikoma, 2008), chemical equilibration of accreting chondritic material (Schaefer and Fegley, 2010), or serpentinization. Then, reduced forms of nitrogen such as NH_3 would be thermochemically favoured near the surface. Once reduced, nitrogen could have become incorporated into ocean sediment and subducted, or dissolved directly into the mantle, if the surface was hot enough to be in a magma ocean state.

To investigate this scenario quantitatively, it is necessary to work out the conditions under which near-surface processes could cause rapid reduction of N_2. Reduced nitrogen in the form of ammonia (NH_3) is highly vulnerable to photolysis by UV radiation in the upper atmosphere (Kuhn and Atreya, 1979), so given low thermochemical conversion rates even a hydrogen-rich atmosphere would have very low surface abundances of reduced nitrogen. To assess the conditions under which equilibrium chemistry would dominate in the lowest part of a highly reducing atmosphere, we first calculate the rate of NH_3 photolysis in the high atmosphere, followed by the rates of thermochemical N reduction as a function of temperature. The question of how reduced atmospheric N is transferred to the mantle is tackled afterwards: the answer turns out to be strongly constrained by the temperatures at which surface reduction of N is effective.

4.1. Destruction of reduced nitrogen by photolysis

An upper bound on the maximum possible global average loss rate of NH_3 from photolysis can be derived from the expression

$$\Phi_{photo,max} = \frac{1}{4}\int_0^{\lambda_{cut}} Q_y(\lambda)\mathcal{F}_\odot(\lambda)\mathrm{d}\lambda, \quad (2)$$

where $\mathcal{F}_\odot(\lambda)$ is the early solar UV flux as a function of wavelength λ, $Q_y(\lambda)$ is the quantum yield of reaction $NH_3 + h\nu \rightarrow NH_2 + H$, λ_{cut} is the wavelength above which the photolysis absorption cross-section of NH_3 drops to negligible values, and the factor 1/4 accounts for averaging over the sphere. Using the best estimate for the XUV/UV spectrum of the Hadean Sun (see below), assumed quantum yield of 1.0 and $\lambda_{cut} = 230$ nm, equation (2) yields 3.8×10^{13} molecules/cm^2/s.

To investigate Hadean NH_3 photolysis in more detail, a photochemical code was constructed. The code solves the 1D partial differential equation

$$\frac{\partial n_i}{\partial t} = P_i - L_i n_i - \frac{\partial \Phi_i}{\partial z}, \quad (3)$$

$$\Phi_i = -\kappa_D n \frac{df_i}{dz} \quad (4)$$

in time on a 100-layer vertical grid that extends from the surface to a height z_{top}, defined here as the altitude where the atmospheric pressure p is 1 Pa. In (3)–(4), n and n_i are the total number density and number density of a given species, respectively, in molecules cm^{-3}, f_i is the molar concentration of a given species, P_i and L_i are chemical production and loss terms, respectively, and κ_D is the (eddy) diffusion coefficient. κ_D was taken to be a constant 1×10^5 cm^2 s^{-1} in some simulations, while in others the present-day κ_D profile from Hunten (1975) was used. Each simulation was run until a steady state was reached ($\partial_t n_i = 0$).

In the model, surface pressure p_s and surface temperature T_s are external parameters. The atmospheric temperature profile is assumed to follow a dry adiabat until the stratospheric temperature T_{strat} is reached. The latter was set to 200 K, close to the skin temperature for an early Earth with decreased solar flux and albedo of ~0.3. Sensitivity tests where a moist adiabat was used for the temperature profile showed only small differences in the column-integrated photolysis rates.

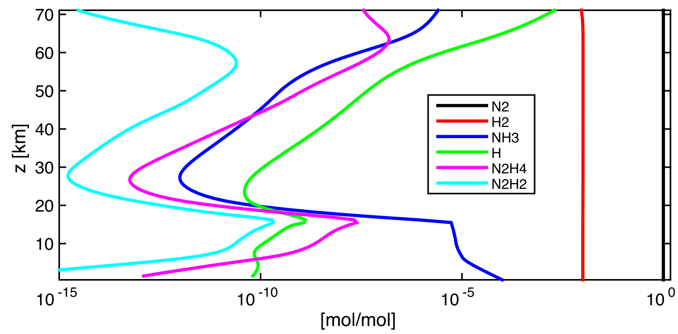

Fig. 2. Example results from the photochemical model. Steady state atmospheric molar concentrations of major species for a N_2-dominated atmosphere. Here $T_s = 300$ K, $p_s = 1$ bar, 10^4 ppmv H_2, surface NH_3 concentration of 100 ppmv, and eddy diffusion and rainout are included based on present-day parameterisations.

To solve (3), a stiff ODE solver from the Fortran DLSODE package is used. For simplicity, the chemical network is restricted in this calculation to N and H species only. A total of 28 N–H reactions are included from various literature sources. Comprehensive calculations involving 4 or more chemical species (C, N, O, H) and 100s of chemical reactions for exoplanet applications indicate that N–H chemistry should dominate the photochemical conversion of NH_3 to N_2 (Venot et al., 2012; Moses, 2014).

We neglect the possibility of ammonia shielding by an organic haze (Sagan and Chyba, 1997). If present, this would allow higher NH_3 buildup, but it would still require a substantial source of CH_4. UV shielding by CO_2 was included in runs where the gas was present. In low temperature simulations, rainout of NH_3 was included in the cool case via a parameterization based on present-day rainfall rates (Kasting, 1982). Rainout removes NH_3 from the high atmosphere and hence decreases photolysis rates. Rayleigh scattering was included using standard parameterisations for N_2 and H_2 (Pierrehumbert, 2010). Because the aim was to derive a lower limit on the total rates of photolysis, the actinic flux contribution was ignored here. This removed the need to perform a multiple scattering calculation.

Photodissociation rates of NH_3, N_2H_4 and H_2 were calculated using an XUV/UV solar spectrum appropriate to 4.2 Ga, with data derived from a combination of direct solar observations and the Sun in Time project (Ribas et al., 2005). The solar zenith angle was set to 60° and a factor of 1/2 applied to the incoming flux to account for diurnal averaging. The model was validated by comparison with the results of previous calculations of NH_3 photolysis for the Archean Earth (Kuhn and Atreya, 1979; Kasting, 1982).

As an example of the model output, Fig. 2 shows steady-state molar concentrations of key species produced for an example case with 1 bar N_2 atmosphere and 1% H_2. As can be seen, NH_3 concentrations decline up to 30 km due to photolysis and rainout, although H_2 photolysis causes f_{NH_3} to increase in the uppermost regions of the atmosphere.

Next, the steady-state ammonia photolysis loss rate (Φ_{loss,NH_3}) was calculated as a function of the surface f_{NH_3} value, which was treated as a fixed parameter in the model. To span the likely range of possibilities, two end-member atmospheric states are modelled: a hot, strongly reducing N_2–H_2 atmosphere, and a cool, weakly reducing N_2–CO_2 atmosphere. As can be seen from Fig. 3, Φ_{loss,NH_3} ranges from just over 1×10^6 to close to $\Phi_{photo,max}$ and is most dependent on the NH_3 surface molar concentration. The calculated minimum value for the hot H_2-rich case is somewhat lower than for the cool N_2–CO_2 case due to NHx radical reactions with H_2, which efficiently recycle photolysed NH_3.

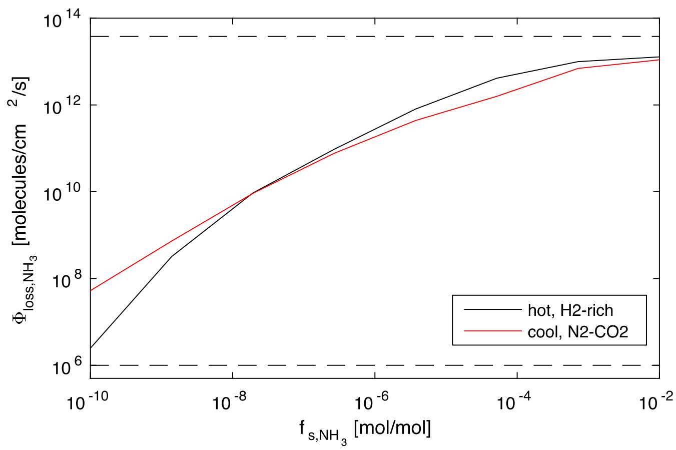

Fig. 3. Predicted ammonia destruction rates as a function of surface NH_3 molar concentration. The black and red lines show results from the photochemical code for a hot hydrogen-rich atmosphere ($f_{H_2} = 0.5$ mol/mol, $f_{N_2} = 0.5$ mol/mol, $T_s = 700$ K, $p_s = 30$ bar) with constant eddy diffusion $\kappa_D = 10^5$ cm^2 s^{-1} and a cool N_2–CO_2 atmosphere ($f_{N_2} = 0.9$ mol/mol, $f_{CO_2} = 0.1$ mol/mol, $T_s = 300$ K, $p_s = 1$ bar) with present-day eddy diffusion profile, respectively. The dashed lines show the upper and lower limits for photolysis rates derived from the results. (For interpretation of the references to colour in this figure legend, the reader is referred to the web version of this article.)

4.2. Production of reduced nitrogen by thermolysis

The final step is to calculate the range of surface temperatures and pressures for which thermochemical equilibrium is approached in the lower atmosphere. This was done by calculating the column-integrated rate of N_2 reduction and comparing directly with the rate of ammonia photolysis. The thermochemistry of nitrogen reduction is still poorly constrained (Moses et al., 2011; Venot et al., 2012), so it was decided not to perform a fully coupled thermokinetic calculation here. Instead, we simply calculate the column-integrated rate of N_2 reduction for fast and slow assumed rate-limiting reactions, and compare the results with the total photolysis rate for a range of surface pressures and temperatures. The rate-limiting reactions used were

$$N_2 + H_2 \longrightarrow NH + NH; \qquad k_2(T) = 8.45 \times 10^{-8} e^{-81515.0/T} \tag{5}$$

and

$$N_2 + H_2 \longrightarrow H_2NN; \qquad k_1(T) = 1.776 \times 10^{-16} T^{1.6} e^{-61580.0/T} \tag{6}$$

for the slow and fast cases, respectively. Rate constants are in units of cm^3 molecule^{-1} s^{-1} in both cases. The rate for (5) is based on experimental data and has been used to study the deep nitrogen cycle on Jupiter (Prinn and Olaguer, 1981), while that for (6) is derived from a fit to ab-initio calculations and has been used in state-of-the-art exoplanet atmospheric modelling (Hwang and Mebel, 2003; Moses et al., 2011).

The maximum column-integrated rate of NH_3 production was assumed to be equal to twice the rate of N_2 thermolysis

$$\Phi_{NH_3,thermo} = 2 \int_0^{z_{top}} n_{N_2}(z) n_{H_2}(z) \mathcal{R}[T(z)] dz \tag{7}$$

where $n_{N_2}(z)$ is the number density of N_2, $n_{H_2}(z)$ is the number density of H_2, $\mathcal{R}[T(z)]$ is the rate of (5) or (6) as a function of temperature and z_{top} is the top of the model atmosphere. To calculate a maximum value, $n_{H_2} = n_{N_2} = 0.5 n_{tot}$ was assumed. In a more realistic situation where the atmosphere was not dominated by equal parts H_2 and N_2, the actual rate of NH_3 production would be lower. The rate of NH_3 production in a coupled model will also be lower than this if the initial reaction of N_2 and H_2 is not the rate-limiting step. In either case, this would increase the temperature and pressure required to achieve balance between surface thermochemical production and atmospheric photochemical destruction of reduced nitrogen. Equation (7) gives a simple upper limit on the efficacy of N_2 reduction by H_2 as a function of atmospheric temperature and pressure.

Fig. 4 (left) shows contour plots of $\Phi_{NH_3,thermo}$ in an H_2-rich atmosphere as a function of surface temperature and pressure. Fig. 4

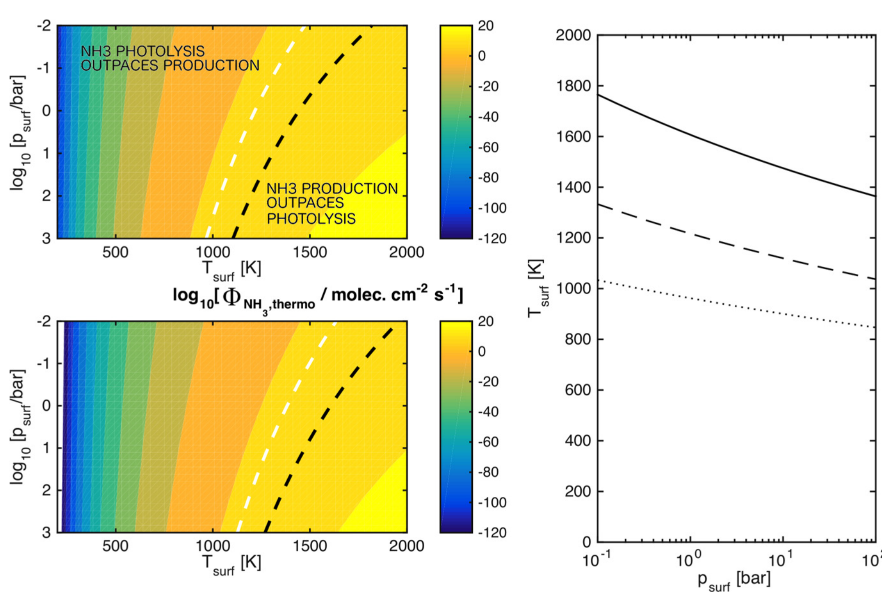

Fig. 4. (left) NH_3 column production rate via atmospheric thermochemistry as a function of surface temperature T_s and surface pressure p_s, assuming that (top) equation (5), (bottom) equation (6) in is the rate-limiting step. The black and white lines show the T_s–p_s curve for which this estimated thermolysis rate equals the maximum and minimum column-integrated NH_3 photolysis rate from the photochemical model, respectively (see Fig. 3). (right) Surface temperature required for ammonia production to outpace photolysis. The solid line is the upper limit assuming slow N_2 thermolysis [reaction (5)] and fast NH_3 photolysis ($\Phi_{loss,NH_3} = \Phi_{photo,max}$) and the dashed line assumes fast N_2 thermolysis [reaction (6)] and slow NH_3 photolysis ($\Phi_{loss,NH_3} = \Phi_{photo,min}$). The dotted line is an extreme lower limit with fast N_2 thermolysis and $\Phi_{loss,NH_3} = \Phi_{photo,min}/10^2$.

(right) shows the surface temperature required for thermochemical production of NH_3 to outpace its photochemical destruction in the atmospheric column, as a function of p_{surf}, for upper and lower limit cases. It can be assumed that above the limiting surface temperature, ammonia concentrations in the low atmosphere will be driven towards chemical equilibrium, which implies molar concentrations of 10–1000 ppm in this temperature range.[2]

As can be seen, for all cases this requires surface temperatures in excess of ∼1000 K, with higher temperatures needed at lower pressures because of the dependence of chemical kinetics on gas density. Even if a NH_3 photolysis rate of only 10^4 molecules/cm^2/s is assumed (the 'extreme lower limit' case in Fig. 4) surface temperatures greater than 800 K are still required, thanks to the extremely high dependence of the rate constants of (5) and (6) on temperature.

Typical solidus temperatures for Earth's mantle are ∼1500 K at 1 bar (Elkins-Tanton, 2012). Hence the key result of this analysis is that conditions approaching those of a magma ocean at the surface are required for reduction of N if gas phase chemistry is the limiting factor. Magma ocean surface conditions on Earth occurred during and just after formation (Matsui and Abe, 1986; Zahnle et al., 2010). The moon-forming impact transformed much of Earth's surface into a molten state (Stewart et al., 2014). The integrated effect of smaller impacts is also sufficient to increase surface temperatures above 1500 K if the thermal blanketing of a H_2O vapour (or H_2) atmosphere is taken into account. Hydrogen absorbs strongly in the infrared above pressures of ~ 0.2 bar due to H_2–H_2 and N_2–H_2 collision-induced absorption, so a thick enough H_2 envelope would provide extremely effective greenhouse warming.[3]

Under magma ocean conditions, reduced atmospheric nitrogen can be transported to the mantle rapidly, because the high Rayleigh numbers typical to magma ocean conditions generally ensure rapid mixing (Solomatov, 2000). In addition, previous experimental work has indicated that nitrogen solubility is greatly increased in reducing magmas and upper mantle minerals (Libourel et al., 2003; Kadik et al., 2011; Li et al., 2013). At relatively high oxygen fugacities (QFM and greater), N_2 is the dominant form of N in the melt, and it behaves similarly to argon, with a solubility of around 0.1 ppmw at 1 bar N_2 pressure (Libourel et al., 2003). As oxygen fugacity decreases to the IW buffer and lower, chemical bonding of N to the silicate melt becomes important and solubility increases by orders of magnitude. Earth's mantle f_{O_2} has been close to the QFM buffer since around 3.8 Ga (Delano, 2001), and perhaps as far back as 4.35 Ga (Trail et al., 2011), but immediately after formation the mantle would have been highly reducing, at the IW buffer or lower (Wade and Wood, 2005). The idea that dissolution of N in an early reducing magma ocean led to significant incorporation of N in the mantle has been proposed previously (e.g., Marty, 2012; Li et al., 2013). The simplicity and robustness of this mechanism compared to the others we have analysed here lead to the conclusion that it is the most plausible explanation for early incorporation of N into the mantle.

4.3. Catalytic effects and CO_2 atmospheres

We have only considered pure N–H chemistry, but catalytic effects could also have been important to Hadean N fixation. Notably, in the Haber process, nitrogen is converted to ammonia in the presence of metallic iron at around 200 bar and 700 K (Erisman et al., 2008). A similar process could have occurred in the Hadean, weakening the surface temperature and pressure requirements. However, the Haber process requires the presence of metallic iron, which in turn implies a crustal oxygen fugacity around the iron–wüstite (IW) buffer or lower. Hence it does not change the basic requirement of a highly reducing surface and atmosphere for abiotic N drawdown.

Similar considerations apply to other catalytic processes such as lightning-driven thermochemistry. Using modern-day rates of energy dissipation by lightning, Chameides and Walker (1981) estimated a peak HCN production rate in the Archean of around 6×10^8 molecules/cm^2/s given an atmosphere with 5% H_2 and C:O ratio greater than 1 (which is extremely reducing). This could lead to drawdown of around 0.6 bar of N_2 in 1 Gy, although the conversion rate of atmospheric HCN to fixed nitrogen in sediment would need to be close to 100% for it to work.

One other possible scenario for the Hadean immediately after the Moon-forming impact involves a thick CO_2 atmosphere (10–100 bar). Under such an atmosphere, a magma ocean could persist for around 10 My, after which time surface temperatures and atmospheric CO_2 levels would likely decline rapidly (Sleep and Zahnle, 2001; Zahnle et al., 2010). A CO_2-dominated atmosphere could shield ammonia from UV photolysis effectively and would cause enhanced ammonia rainout rates by decreasing raindrop pH. It would also decrease ocean pH levels, probably to the extent where most ammonia in the atmosphere–ocean system would be converted to aqueous NH_4^+. For rapid N drawdown to occur in this scenario, however, an efficient abiotic means of reducing N_2 in the first place is still required.

5. Nitrogen equilibration on Venus: the water loss redox pump

If a Hadean abiotic process is the explanation for Earth's atmosphere–mantle nitrogen partitioning, the above analysis should also apply to other planets. The case of Venus is particularly interesting, because Venus is similar in size to Earth, but it possesses around 3.4 times as much nitrogen in its atmosphere scaled by mass (Hoffman et al., 1980; Goldblatt et al., 2009). What could explain the difference?

The most obvious difference between Earth and Venus is their distance to the Sun. Because it receives a greater solar flux, Venus most likely passed through a runaway greenhouse phase, either immediately after its formation (Gillmann et al., 2009; Hamano et al., 2013) or later on, once the solar luminosity increased past a critical threshold (Ingersoll, 1969). In either case, extensive water loss accompanied by buildup of oxygen in the atmosphere would have been the result. The abundance of O_2 in the Venusian atmosphere today is <3 ppm (Mills, 1999), so the vast majority of this oxygen must have been absorbed by the crust and mantle.

The redox state of the Venusian crust is close to the magnetite–hematite boundary based on spectroscopic observations of surface minerals by the Venera spacecraft (Florensky et al., 1983; Fegley et al., 1997). Because Venus underwent a major resurfacing event ca. 0.3 Ga (Strom et al., 1994) and hydrogen loss rates in the present era are low ($\sim 1 \times 10^{26}$ atoms/s, or 1.0×10^{-5} terrestrial oceans in the last 0.3 Gy) (Lammer et al., 2006), the Venusian surface redox state should be close to that of its mantle. In contrast, the oxygen fugacity of Earth's upper mantle is closer to the more reducing QFM buffer.

[2] Based on gas phase equilibrium calculations using the online NASA CEA database (http://cearun.grc.nasa.gov/).

[3] An approximate estimate of the equilibrium surface temperature for an H_2-dominated atmosphere can be given by $T_s = T_e(p_s/p_e)^{R/c_p}$ where R is the specific gas constant, c_p is the specific heat capacity at constant volume, T_e is the emission temperature, p_e is the emission pressure (around 0.2 bar for H_2) and p_s is surface pressure. Taking T_e to be the equilibrium temperature given albedo $A = 0.3$ and a faint young Sun ($T_e = 235$ K), and $R/c_p = 0.289$, we get $T_s = 1000$ K for around 30 bar of H_2. Detailed radiative–convective calculations (results not shown) indicate that when H_2O is included the required pressure is around 100 bars of H_2 for planetary albedos in the range 0.3–0.7, due to the effect of moist convection on the adiabatic lapse rate.

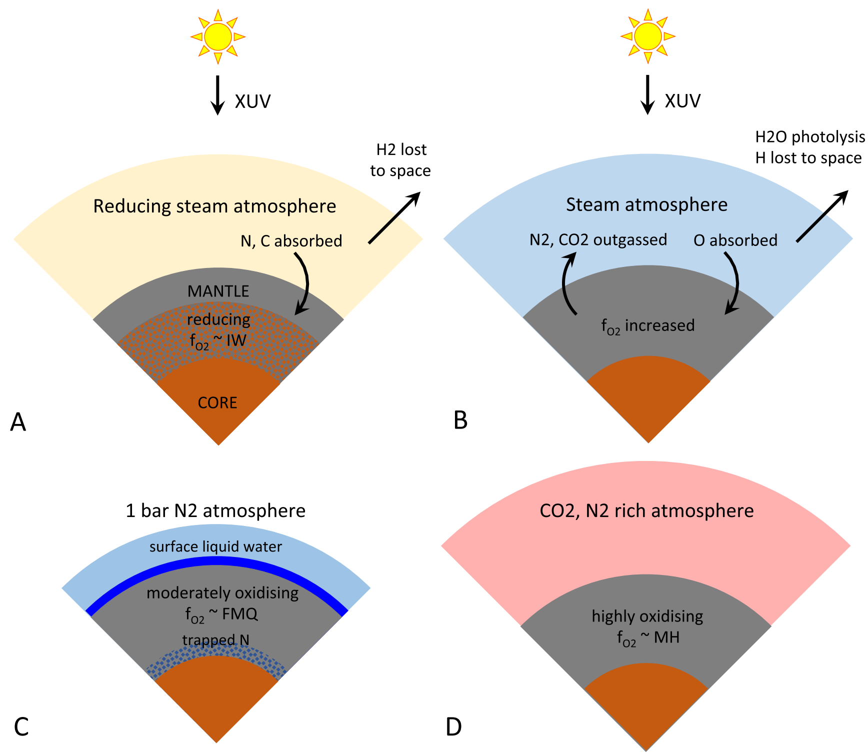

Fig. 5. Schematic of the water loss redox pump explanation for the differing atmospheric N_2 inventories of Earth and Venus. Both planets start in state A. Earth evolves directly to state C, whereas Venus passes through state B before ending up in D. See text for full description.

Based on these observations, we can propose the following explanation for the difference in Venus and Earth's atmospheric nitrogen inventories. Both planets have highly reducing steam atmospheres (state A in Fig. 5) during and shortly after formation. Earth cools relatively rapidly and forms liquid oceans, passing to state C: a planet with around 1 bar of atmospheric N_2, smaller amounts of atmospheric H_2, and a moderately oxidising mantle. In the terminology of Hamano et al. (2013), it is a Type I planet. In contrast, Venus undergoes a sustained runaway greenhouse phase (state B), leading to extensive photolysis of H_2O followed by loss of hydrogen to space. The oxygen liberated from H_2O photolysis is then absorbed by the mantle, raising its oxygen fugacity and expelling nitrogen into the atmosphere as a result. The end state is a dry planet with a greater atmospheric N_2 inventory (state D).

An estimate of the total oxidation of Venus during an early period of H_2O photolysis can be made by noting that in the Sun's saturated phase of XUV emission, which probably lasted around 100 My (Ribas et al., 2005), XUV levels would have been high enough to drag oxygen along with the escaping hydrogen (Zahnle and Kasting, 1986; Chassefière, 1996). In this escape regime, the rate of oxygen buildup is approximately determined by the diffusion of O atoms downwards from the upper atmosphere (e.g., Luger and Barnes, 2015), with the flux given by

$$\Phi_O \approx \frac{5bm_H g}{k_B T}. \tag{8}$$

Here m_H is the mass of one hydrogen atom, g is Venusian gravity in the upper atmosphere, k_B is Boltzmann's constant, T is the temperature of the atmosphere in the region of peak diffusion and $b = b(T)$ is the binary diffusion coefficient for O in H (Zahnle, 1986). Assuming $T \approx 300$–600 K, $\Phi_O \approx 3.8$–7.6×10^{12} molecules/cm^2/s. Hence 1.2–2.4 terrestrial oceans (TO) worth of oxygen could have been liberated from H_2O on Venus during the first 100 My. For comparison, Earth's estimated total H_2O inventory is of order 1–4 TO (Hirschmann, 2006).

How much liberated O is necessary to change the oxidation state of the mantle? If Venus' early upper mantle was 10% of the total planetary mass and contained 5 wt% iron in the form of FeO, oxidation of all of the FeO to hematite ($2FeO + 0.5O_2 \rightarrow Fe_2O_3$) would require 2.8 TO, given that 1 TO is 7.8×10^{22} moles O. This is a lot of oxygen. However, the amount of water loss required to affect early nitrogen partitioning will be lower than this value. First, just after formation the redox state of rocky planet mantles is below even the IW buffer (Wade and Wood, 2005). In the absence of buffering by an abundant element such as Fe, much lower levels of O buildup will then lead to significant mantle f_{O_2} changes. Differences of 1–2 in $\log_{10} f_{O_2}$ below the IW buffer cause variations in N solubility of 0.1–10 ppm at 1 bar (Libourel et al., 2003). In early highly reducing conditions, therefore, the oxidation of Venus due to water loss would have a much greater effect than later on. Second, planetary interiors are highly heterogeneous. If water loss on early Venus led to mixing of highly oxidised surface material with reduced, N-rich material in the deep interior, this could also cause increased outgassing of N over time even if the oxidation state of the upper mantle remained constant. Increased oxidation via water loss hence appears easily capable of explaining the 3.4× greater atmospheric inventory of Venus compared to the Earth.

Alternative explanations for the differing atmospheric N inventories of Earth and Venus involving delivery or escape processes are possible, but less compelling. Venus has atmospheric Ne and ^{36}Ar abundances several tens of times greater than Earth, suggesting that it captured a larger component of the nebula during formation (Wieler, 2002). However, this nebular addition cannot have increased Venus' total atmospheric nitrogen inventory significantly. There is approximately 3.2×10^{17} mol of ^{36}Ar in the Venusian atmosphere vs. 3.7×10^{20} mol of N_2 (Hoffman et al., 1980; Wieler, 2002; Lodders, 2003). The N/^{36}Ar molar ratio in the solar photosphere is around 22.4, which implies that a maximum of about 1.0% of Venus's atmospheric nitrogen could have a nebular origin. This is consistent with Venus' essentially chondritic ^{15}N/^{14}N ratio, which suggests the bulk of its nitrogen was supplied from the same source as Earth's (Hunten, 1983).

Regarding loss processes, Venus' closer proximity to the Sun means that its early XUV-driven escape rates were greater than Earth's, both for hydrogen and potentially for N via hydrodynamic drag (Chassefière, 1996). Earth underwent the Moon-forming impact, which could have removed a substantial portion of the atmosphere, depending on factors such as the initial angular momentum of the protoearth and presence/absence of an ocean (Genda and Abe, 2005; Ćuk and Stewart, 2012). However, Venus must also have lost significant amounts of its atmosphere to space by impact erosion during the late stages of its formation. In addition, impact-driven loss of N_2 to space from Earth after the Moon-forming impact would cause loss of noble gases such as ^{36}Ar by the same proportion. However as mentioned in the Introduction, Earth is depleted in atmospheric N vs. noble gases relative to chondritic material. This suggests extensive loss of N to space on Earth as an explanation for its lower atmospheric N inventory vs. Venus is also problematic, unless Earth's noble gas inventory is dominated by a late cometary contribution (Marty, 2012).

6. Conclusion

Taken together, the existing geological constraints on Earth's nitrogen present a paradox: large amounts of N appear to be present in the mantle, there is a high present-day flux to the mantle from the surface, but the amount of N_2 in the atmosphere has not changed significantly since 3–3.5 Ga. There are several possible resolutions to this problem. The first is that some of the observations are incorrect. In future, study of a wider range of proxies for paleopressure over multiple eras and more detailed investigation of heterogeneity in present-day fluxes and reservoirs will be necessary to eliminate this possibility.

Starting from the assumption that the latest constraints on paleopressure and mantle N inventory are correct, we have considered a range of possible mechanisms for nitrogen drawdown in Earth's early history. It has been shown that for multiple reasons, biologically driven subduction of bars of nitrogen in the early Archean is unlikely. Instead, by far the most effective way to fix atmospheric N rapidly is via direct reduction in a hot Hadean atmosphere. Hence if p_{N_2} was indeed low 3–3.5 Ga, Earth's mantle N must have been emplaced early, when conditions were extremely hot and reducing. The simplest way for this to occur is via direct diffusion into a magma ocean, when atmospheric-interior exchange rates would have been rapid. A new redox pump mechanism has been proposed that can naturally explain the differences in atmospheric N inventory between Venus and Earth via enhanced mantle oxidation following water loss in this scenario.

Interestingly, Mars has an extremely low atmospheric N inventory ($\sim 5 \times 10^{-8}$ wt% of the total mass, vs. 6.7×10^{-5} wt% for Earth) (Mahaffy et al., 2013). Escape to space goes some way towards explaining the difference, but may not account for all of it (Jakosky et al., 1994). The topmost region of Mars' surface is highly oxidised, but Mars' low received solar flux prohibits a long-lived early steam atmosphere after formation. Indeed, the oxygen fugacity of the Martian mantle is even lower than that of Earth (Wadhwa, 2001), possibly as a result of its smaller size and rapid core formation (Wade and Wood, 2005). Storage in the mantle may therefore also help explain Mars' nitrogen-poor atmosphere.

The results described here have several important wider implications. The redox pump explanation for Venus' nitrogen inventory has implications for predicting the evolution of other volatiles (e.g. carbon) both on Venus and on close-in, low mass exoplanets such as Gliese 1132b (Berta-Thompson et al., 2015). It is also testable, in principle, by future in situ measurements of the N inventory of the Venusian crust. In addition, if an early reducing atmosphere is necessary to explain Earth's nitrogen budget, this has implications for prebiotic chemistry and the emergence of life. Future theoretical studies should investigate these implications in more detail.

Acknowledgements

The author thanks Eric Hebrard for his advice and sharing of reaction rate data during construction of the photochemical code and the anonymous reviewers for their comments, which greatly improved the quality of the paper. This manuscript has benefited from conversations with many researchers, including N. Dauphas, A. Knoll, H. Lammer, B. Marty, A. Pearson, D. Schrag and K. Zahnle.

Appendix A. Supplementary material

Supplementary material related to this article can be found online at http://dx.doi.org/10.1016/j.epsl.2016.04.002.

References

Battistuzzi, F.U., Feijao, A., Hedges, S.B., 2004. A genomic timescale of prokaryote evolution: insights into the origin of methanogenesis, phototrophy, and the colonization of land. BMC Evol. Biol. 4, 44–57.
Berta-Thompson, Z.K., Irwin, J., Charbonneau, D., Newton, E.R., Dittmann, J.A., Astudillo-Defru, N., Bonfils, X., Gillon, M., Jehin, E., Stark, A.A., Stalder, B., Bouchy, F., Delfosse, X., Forveille, T., Lovis, C., Mayor, M., Neves, V., Pepe, F., Santos, N.C., Udry, S., Wünsche, A., 2015. A rocky planet transiting a nearby low-mass star. Nat. Geosci. 527 (7577), 204–207.
Bjerrum, C.J., Canfield, D.E., 2002. Ocean productivity before about 1.9 gyr ago limited by phosphorus adsorption onto iron oxides. Nature 417 (6885), 159–162.
Bjerrum, C.J., Canfield, D.E., 2004. New insights into the burial history of organic carbon on the early Earth. Geochem. Geophys. Geosyst. 5 (8).
Blank, C.E., 2009. Not so old Archaea – the antiquity of biogeochemical processes in the archaeal domain of life. Geobiology 7, 495–514.
Busigny, V., Bebout, G., 2013. Nitrogen in the silicate earth: speciation and isotopic behavior during mineral–fluid interactions. Elements 9 (5), 353–358.
Cartigny, P., Marty, B., 2013. Nitrogen isotopes and mantle geodynamics: the emergence of life and the atmosphere–crust–mantle connection. Elements 9 (5), 359–366.
Chameides, W.L., Walker, J., 1981. Rates of fixation by lightning of carbon and nitrogen in possible primitive atmospheres. Orig. Life Evol. Biosph. 11 (4), 291–302.
Chassefière, E., 1996. Hydrodynamic escape of hydrogen from a hot water-rich atmosphere: the case of Venus. J. Geophys. Res. 101, 26039–26056.
Ćuk, M., Stewart, S.T., 2012. Making the Moon from a fast-spinning earth: a giant impact followed by resonant despinning. Science 338 (6110), 1047–1052.
Delano, J.W., 2001. Redox history of the Earth's interior since 3900 ma: implications for prebiotic molecules. Orig. Life Evol. Biosph. 31 (4–5), 311–341.
Des Marais, D.J., Strauss, H., Summons, R.E., Hayes, J., 1992. Carbon isotope evidence for the stepwise oxidation of the Proterozoic environment. Nature 359, 605–609.
Dhuime, B., Hawkesworth, C.J., Cawood, P.A., Storey, C.D., 2012. A change in the geodynamics of continental growth 3 billion years ago. Science 335 (6074), 1334–1336.
Elkins-Tanton, L.T., 2012. Magma oceans in the inner solar system. Annu. Rev. Earth Planet. Sci. 40, 113–139.
Erisman, J.W., Sutton, M.A., Galloway, J., Klimont, Z., Winiwarter, W., 2008. How a century of ammonia synthesis changed the world. Nat. Geosci. 1 (10), 636–639.
Fegley Jr., B., Zolotov, M.Y., Lodders, K., 1997. The oxidation state of the lower atmosphere and surface of Venus. Icarus 125 (2), 416–439.
Filippelli, G.M., 2008. The global phosphorus cycle: past, present, and future. Elements 4 (2), 89–95.
Flament, N., Coltice, N., Rey, P.F., 2008. A case for late-Archaean continental emergence from thermal evolution models and hypsometry. Earth Planet. Sci. Lett. 275 (3), 326–336.
Florensky, C., Nikolaeva, O., Volkov, V., Kudryashova, A., Pronin, A., Gektin, Y.M., Tchaikina, E., Bashkirova, A., 1983. Redox indicator "contrast" on the surface of Venus. In: Lunar and Planetary Science Conference, vol. 14, pp. 203–204.
Geider, R., La Roche, J., 2002. Redfield revisited: variability of C:N:P in marine microalgae and its biochemical basis. Eur. J. Phycol. 37 (1), 1–17.
Genda, H., Abe, Y., 2005. Enhanced atmospheric loss on protoplanets at the giant impact phase in the presence of oceans. Nature 433 (7028), 842–844.
Genda, H., Ikoma, M., 2008. Origin of the ocean on the Earth: early evolution of water D/H in a hydrogen-rich atmosphere. Icarus 194 (1), 42–52.
Gillmann, C., Chassefière, E., Lognonné, P., 2009. A consistent picture of early hydrodynamic escape of Venus atmosphere explaining present Ne and Ar isotopic ratios and low oxygen atmospheric content. Earth Planet. Sci. Lett. 286, 503–513.

Goldblatt, C., Claire, M.W., Lenton, T.M., Matthews, A.J., Watson, A.J., Zahnle, K.J., 2009. Nitrogen-enhanced greenhouse warming on early Earth. Nat. Geosci. 2, 891–896.
Halliday, A.N., 2013. The origins of volatiles in the terrestrial planets. Geochim. Cosmochim. Acta 105, 146–171.
Hamano, K., Abe, Y., Genda, H., 2013. Emergence of two types of terrestrial planet on solidification of magma ocean. Nature 497 (7451), 607–610.
Hirschmann, M.M., 2006. Water, melting, and the deep Earth H_2O cycle. Annu. Rev. Earth Planet. Sci. 34, 629–653.
Hoffman, J.H., Hodges, R.R., Donahue, T.M., McElroy, M.B., 1980. Composition of the Venus lower atmosphere from the pioneer Venus mass spectrometer. J. Geophys. Res., Space Phys. (1978–2012) 85 (A13), 7882–7890.
Hunten, D.M., 1975. Vertical transport in atmospheres. In: Atmospheres of Earth and the Planets. Springer, pp. 59–72.
Hunten, D.M. (Ed.), 1983. Venus. University of Arizona Press.
Hwang, D.-Y., Mebel, A.M., 2003. Reaction mechanism of N_2/H_2 conversion to NH_3: a theoretical study. J. Phys. Chem. A 107 (16), 2865–2874.
Ingersoll, A.P., 1969. The runaway greenhouse: a history of water on Venus. J. Atmos. Sci. 26, 1191–1198.
Jakosky, B.M., Pepin, R.O., Johnson, R.E., Fox, J.L., 1994. Mars atmospheric loss and isotopic fractionation by solar-wind-induced sputtering and photochemical escape. Icarus 111 (2), 271–288.
Johnson, B., Goldblatt, C., 2015. The nitrogen budget of Earth. Earth-Sci. Rev. 148, 150–173.
Kadik, A., Kurovskaya, N., Ignat'ev, Y.A., Kononkova, N., Koltashev, V., Plotnichenko, V., 2011. Influence of oxygen fugacity on the solubility of nitrogen, carbon, and hydrogen in $FeO–Na_2O–SiO_2–Al_2O_3$ melts in equilibrium with metallic iron at 1.5 GPa and 1400 °C. Geochem. Int. 49 (5), 429–438.
Kasting, J.F., 1982. Stability of ammonia in the primitive terrestrial atmosphere. J. Geophys. Res., Oceans 87 (C4), 3091–3098.
Kharecha, P., Kasting, J., Siefert, J., 2005. A coupled atmosphere-ecosystem model of the early Archean Earth. Geobiology 3, 53–76.
Knowles, C.J., 1988. Cyanide utilization and degradation by microorganisms. Cyanide Compd. Biol. 140, 3–15.
Kuhn, W.R., Atreya, S.K., 1979. Ammonia photolysis and the greenhouse effect in the primordial atmosphere of the Earth. Icarus 37 (1), 207–213.
Lammer, H., Lichtenegger, H., Biernat, H., Erkaev, N., Arshukova, I., Kolb, C., Gunell, H., Lukyanov, A., Holmstrom, M., Barabash, S., et al., 2006. Loss of hydrogen and oxygen from the upper atmosphere of Venus. Planet. Space Sci. 54 (13), 1445–1456.
Li, Y., Wiedenbeck, M., Shcheka, S., Keppler, H., 2013. Nitrogen solubility in upper mantle minerals. Earth Planet. Sci. Lett. 377, 311–323.
Libourel, G., Marty, B., Humbert, F., 2003. Nitrogen solubility in basaltic melt. Part I. Effect of oxygen fugacity. Geochim. Cosmochim. Acta 67 (21), 4123–4135.
Lodders, K., 2003. Solar system abundances and condensation temperatures of the elements. Astrophys. J. 591 (2), 1220.
Luger, R., Barnes, R., 2015. Extreme water loss and abiotic O_2 buildup on planets throughout the habitable zones of *m* dwarfs. Astrobiology 15 (2), 119–143.
Mahaffy, P.R., Webster, C.R., Atreya, S.K., Franz, H., Wong, M., Conrad, P.G., Harpold, D., Jones, J.J., Leshin, L.A., Manning, H., et al., 2013. Abundance and isotopic composition of gases in the martian atmosphere from the Curiosity rover. Science 341 (6143), 263–266.
Marty, B., 1995. Nitrogen content of the mantle inferred from N_2–Ar correlation in oceanic basalts. Nature 377 (6547), 326–329.
Marty, B., 2012. The origins and concentrations of water, carbon, nitrogen and noble gases on Earth. Earth Planet. Sci. Lett. 313, 56–66.
Marty, B., Dauphas, N., 2003. The nitrogen record of crust–mantle interaction and mantle convection from Archean to present. Earth Planet. Sci. Lett. 206 (3), 397–410.
Marty, B., Zimmermann, L., Pujol, M., Burgess, R., Philippot, P., 2013. Nitrogen isotopic composition and density of the Archean atmosphere. Science 342 (6154), 101–104.
Matsui, T., Abe, Y., 1986. Evolution of an impact-induced atmosphere and magma ocean on the accreting Earth. Nature 319, 303–305.
Mills, F.P., 1999. A spectroscopic search for molecular oxygen in the Venus middle atmosphere. J. Geophys. Res., Planets (1991–2012) 104 (E12), 30757–30763.
Moses, J.I., 2014. Chemical kinetics on extrasolar planets. Philos. Trans. R. Soc. London A, Math. Phys. Eng. Sci. 372, 20130073.
Moses, J.I., Visscher, C., Fortney, J.J., Showman, A.P., Lewis, N.K., Griffith, C.A., Klippenstein, S.J., Shabram, M., Friedson, A.J., Marley, M.S., et al., 2011. Disequilibrium carbon, oxygen, and nitrogen chemistry in the atmospheres of HD 189733b and HD 209458b. Astrophys. J. 737 (1), 15.
Owen, T., Mahaffy, P.R., Niemann, H.B., Atreya, S., Wong, M., 2001. Protosolar nitrogen. Astrophys. J. Lett. 553 (1), L77.
Pavlov, A.A., Hurtgen, M.T., Kasting, J.F., Arthur, M.A., 2003. Methane-rich Proterozoic atmosphere? Geology 31 (1), 87–90.
Pierrehumbert, R., 2010. Principles of Planetary Climate. Cambridge University Press.
Prinn, R.G., Olaguer, E.P., 1981. Nitrogen on Jupiter: a deep atmospheric source. J. Geophys. Res., Oceans 86 (C10), 9895–9899.
Ribas, I., Guinan, E.F., Güdel, M., Audard, M., 2005. Evolution of the solar activity over time and effects on planetary atmospheres. I. High-energy irradiances (1–1700 Å). Astrophys. J. 622, 680–694.
Sagan, C., Chyba, C., 1997. The early faint sun paradox: organic shielding of ultraviolet-labile greenhouse gases. Science 276 (5316), 1217–1221.
Sagan, C., Mullen, G., 1972. Earth and Mars: evolution of atmospheres and surface temperatures. Science 177, 52–56.
Schaefer, L., Fegley, B., 2010. Chemistry of atmospheres formed during accretion of the Earth and other terrestrial planets. Icarus 208 (1), 438–448.
Schrag, D.P., Higgins, J.A., Macdonald, F.A., Johnston, D.T., 2013. Authigenic carbonate and the history of the global carbon cycle. Science 339 (6119), 540–543.
Sleep, N.H., Zahnle, K., 2001. Carbon dioxide cycling and implications for climate on ancient Earth. J. Geophys. Res. 106, 1373–1400.
Solomatov, V.S., 2000. Fluid dynamics of a terrestrial magma ocean. Origin of the Earth and Moon, vol. 1, pp. 323–338.
Som, S.M., Catling, D.C., Harnmeijer, J.P., Polivka, P.M., Buick, R., 2012. Air density 2.7 billion years ago limited to less than twice modern levels by fossil raindrop imprints. Nature 484 (7394), 359–362.
Stewart, S., Lock, S., Mukhopadhyay, S., 2014. Partial atmospheric loss and partial mantle melting during the giant impact stage of planet formation. In: 45th Lunar and Planetary Science Conference.
Strom, R.G., Schaber, G.G., Dawson, D.D., 1994. The global resurfacing of Venus. J. Geophys. Res., Planets (1991–2012) 99 (E5), 10899–10926.
Tian, F., Kasting, J., Zahnle, K., 2011. Revisiting HCN formation in Earth's early atmosphere. Earth Planet. Sci. Lett. 308 (3), 417–423.
Trail, D., Watson, E.B., Tailby, N.D., 2011. The oxidation state of hadean magmas and implications for early Earth's atmosphere. Nature 480 (7375), 79–82.
Tyburczy, J.A., Frisch, B., Ahrens, T.J., 1986. Shock-induced volatile loss from a carbonaceous chondrite: implications for planetary accretion. Earth Planet. Sci. Lett. 80 (3), 201–207.
Venot, O., Hébrard, E., Agùndez, M., Dobrijevic, M., Selsis, F., Hersant, F., Iro, N., Bounaceur, R., 2012. A chemical model for the atmosphere of hot Jupiters. Astron. Astrophys. 546.
Wade, J., Wood, B., 2005. Core formation and the oxidation state of the Earth. Earth Planet. Sci. Lett. 236 (1), 78–95.
Wadhwa, M., 2001. Redox state of Mars' upper mantle and crust from Eu anomalies in shergottite pyroxenes. Science 291 (5508), 1527–1530.
Wieler, R., 2002. Noble gases in the solar system. Rev. Mineral. Geochem. 47 (1), 21–70.
Wordsworth, R., Pierrehumbert, R., 2013. Hydrogen–nitrogen greenhouse warming in Earth's early atmosphere. Science 339 (6115), 64–67.
Wordsworth, R., Pierrehumbert, R., 2014. Abiotic oxygen-dominated atmospheres on terrestrial habitable zone planets. Astrophys. J. Lett. 785 (2), L20.
Yung, Y.L., Allen, M., Pinto, J.P., 1984. Photochemistry of the atmosphere of Titan: comparison between model and observations. Astrophys. J. Suppl. Ser. 55, 465–506.
Zahnle, K., Schaefer, L., Fegley, B., 2010. Earth's earliest atmospheres. Cold Spring Harb. Perspect. Biol. 2 (10).
Zahnle, K.J., 1986. Photochemistry of methane and the formation of hydrocyanic acid (HCN) in the Earth's early atmosphere. J. Geophys. Res., Atmos. (1984–2012) 91 (D2), 2819–2834.
Zahnle, K.J., Kasting, J.F., 1986. Mass fractionation during transonic escape and implications for loss of water from Mars and Venus. Icarus 68 (3), 462–480.